Catalysis Science & Technology

ROYAL SOCIETY OF CHEMISTRY

PAPER

View Article Online
View Journal | View Issue

Cite this: *Catal. Sci. Technol.*, 2021, 11, 2292

g-C_3N_4/metal halide perovskite composites as photocatalysts for singlet oxygen generation processes for the preparation of various oxidized synthons†

Marco Corti,[a] Rossella Chiara,[a] Lidia Romani,[a] Barbara Mannucci,[b] Lorenzo Malavasi*[a] and Paolo Quadrelli *[a]

Received 7th December 2020,
Accepted 15th January 2021

DOI: 10.1039/d0cy02352c

rsc.li/catalysis

g-C_3N_4/metal halide perovskite composites were prepared and used for the first time as photocatalysts for *in situ* $^1O_2$ generation to perform hetero Diels–Alder, ene and oxidation reactions with suitable dienes and alkenes. The standardized methodology was made applicable to a variety of olefinic substrates. The scope of the method is finely illustrated and the reactions afforded desymmetrized hydroxy-ketone derivatives, unsaturated ketones and epoxides. Some limitations were also observed, especially in the case of the alkene oxidations, and poor chemoselectivity was somewhere observed in this work which is the first application of MHP-based composites for *in situ* $^1O_2$ generation. The experimental protocol can be used as a platform to further expand the knowledge and applicability of MHPs to organic reactions, since perovskites offer a rich variety of tuning strategies which may be explored to improve reaction yields and selectivities.

Introduction

Singlet oxygen ($^1O_2$)[1–4] is a highly reactive and short-lived oxygen species and can undergo a variety of reactions; among them, the hetero Diels–Alder (HDA) [4 + 2] cycloadditions, the [2 + 2] cycloadditions, the ene reactions and epoxidations are representative of the most interesting ways to afford valuable synthons to be used in remarkable approaches toward organic molecules.[5–8] Photocatalysis uses light and pure oxygen to insert oxygenated functionalities on a carbon skeleton, avoiding the use of, in some cases, extremely toxic heavy metal catalysts; for these and other reasons, photocatalysis is an intrinsically environment friendly methodology.

$^1O_2$ is photochemically produced by the use of organic molecules (sensitizers)[9] or, alternatively, through classical hydrogen peroxide decomposition promoted by hypochlorite or hypobromite and ozonide decomposition. Moreover, $^1O_2$ can also be obtained by thermal decomposition of unstable molecules, such as arene endoperoxides, or by photolysis of oxone.[10] These methodologies are not devoid of problems due essentially to the instability of the organic sensitizers or not completely applicable to the experimental conditions required by specific syntheses. For these reasons, the modern chemical literature on $^1O_2$ reports the photochemical properties of new catalytic systems that proved to be nicely applicable to the generation of such transient oxygen species.

For example, the use of a Pd-conjoined metallosquare with encapsulated fullerenes produces an efficient and photochemically stable $^1O_2$ photosensitizer. The metallocage with the encapsulated fullerenes can oxidize a series of cyclic and acyclic alkenes at room temperature *via* visible light. These reactions take advantage of the excellent spin-converting properties of fullerenes, which makes them excellent agents for $^1O_2$ production.[11]

The need for oxygen-containing heterocycles or simply oxidized organic synthons is a continuous growing task in organic synthesis.[12] A range of products were obtained from the photo-oxidation of cyclopentadiene from photochemically generated $^1O_2$ using carbon dioxide (CO_2) as a solvent and 5,10,15,20-tetrakis(pentafluorophenyl)porphyrin (TPFPP) as a CO_2-soluble photosensitizer. The endoperoxide intermediate was transformed into one of several different products in good yield depending on the conditions applied and by adding different reactors and reagents downstream of the photo-reactor, allowing the reaction products to be switched in one streamlined process. Quite remarkably, quenching with thiourea yielded the *syn*-diol, (1*R*,3*S*)-cyclopent-4-ene-1,3-

[a] *University of Pavia, Department of Chemistry, Viale Taramelli 12, 27100 – Pavia, Italy. E-mail: lorenzo.malavasi@unipv.it, paolo.quadrelli@unipv.it*
[b] *University of Pavia, Centro Grandi Strumenti (CGS), Via Bassi 21, 27100 – Pavia, Italy*

† Electronic supplementary information (ESI) available. See DOI: 10.1039/d0cy02352c

diol, a valuable synthon for a variety of natural products. Treatment with an acid or a base afforded furfuryl alcohol and 4-hydroxy-2-cyclopentenone, respectively. High productivities for all products were obtained when compared to traditional batch reactions.[13,14]

Moreover, continuous flow photooxidation of several conjugated dienes and subsequent rearrangement were engineered, involving endoperoxidation, Kornblum–DeLaMare rearrangement, and additional rearrangements to obtain useful hydroxyenones, furans, and 1,4-dicarbonyl building blocks.[8]

In this panorama, recently, we entered this challenging competition for $^1O_2$ generation easy methods by proposing the catalytic use of oxidized graphitic carbon nitride (g-C_3N_4) for $^1O_2$ generation under photochemical conditions. Some HDA and ene reactions were conducted on selected dienes and alkenes showing a general ability of oxidized g-C_3N_4 to promote chemoselective and unselective oxidative processes with strong dependence on substrate nature (Fig. 1). The results offer a good picture of the ability of this type of catalyst to be employed in organic reactions to prepare valuable synthons that can be used in several value-added preparations.[15] Tuning of the oxidative properties of suitably modified g-C_3N_4 has a pivotal role in determining a sustainable change in the approach to $^1O_2$ generation methods, allowing for greener ways to perform organic reactions.

g-C_3N_4, a polymeric semiconductor, consisting of 6-membered rings with sp^2-nature bonds between the C and N atoms, is prepared by bulk and hard template pyrolysis of melamine (MLM) or, alternatively, from other carbon/nitrogen containing sources (*e.g.* urea). The large possibilities for its functionalization and controlling its catalytic activity make g-C_3N_4 a very promising material for the development of new solar-driven ecologically-friendly reactions.[16] It must be noted that g-C_3N_4 is the most stable allotropic form of carbon nitride and possesses unique electronic properties as well as catalytic and photocatalytic activity.[17]

Upon pursuing our interest in finding new and greener methods for $^1O_2$ generation, as well as sustainable applications in the synthesis of valuable organic intermediates, we wish to report here our recent results concerning $^1O_2$ generation through a variety of modified g-C_3N_4 catalysts in the presence of metal halide perovskites (MHPs), thus forming a heterojunction composite. In particular, we have recently reported the favorable coupling of a lead-free 2D MHP, namely PEA_2SnBr_4, with g-C_3N_4 for hydrogen photogeneration, demonstrating the synergic effect of coupling the two semiconductors in such a catalytic system.[18–20] Considering the superior optical properties of MHPs, particularly the reduced charge carrier recombination and the strong absorbance, it is an extremely appealing strategy to create novel catalytic systems where MHPs improve the efficiency of traditional materials such as graphitic carbon nitride through the formation of a heterojunction composite. For these reasons, in the present work, we exploited the possible application of various catalytic systems, most of them already tested by our group for hydrogen photogeneration, composed of 2D or 3D MHPs, coupled to g-C_3N_4, to investigate the scope of the method in HDA, ene and oxidation reactions with representative dienes and alkenes. We increased the number of substrates used to perform the reactions and found interesting as well valuable limitations occurring with some of them. The obtained value-added compounds are commonly the synthons for a remarkably high range of synthetic transformations, widely applied in modern organic synthesis and here derived from a sustainable and greener $^1O_2$ methodology in organic synthesis taking advantage of easily tunable catalysts.

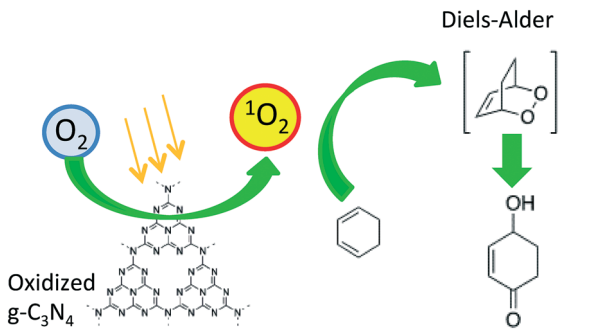

Fig. 1 $^1O_2$ generation from oxidized g-C_3N_4 and application in HDA cycloaddition reaction (upon permission from *ACS Sustainable Chem. Eng.* 2019, **7**, 8176–8182).

Results and discussion

We have prepared g-C_3N_4/PEA_2MX_4 (PEA = phenylethylammonium; M = Pb and Sn; X = Br and Cl) composites at 5 wt% metal halide perovskite loadings (Table 1, entries 1–3) and g-C_3N_4/$DMASnBr_3$ (DMA = dimethylammonium; Table 1, entry 4) by adapting known methodologies.[18,19] As mentioned above, such composites have been selected based on their favorable photocatalytic activity shown in hydrogen generation and organic pollutant degradation.[18–20] Such preliminary evidence suggests their possible exploitation in other catalysis fields as pursued in the present work. Details on the preparation and characterization of the g-C_3N_4/metal halide perovskite composites have been already reported by our group.[18,19]

Table 1 reports all the formulas of the catalysts with the corresponding labeling. To optimize the reaction conditions, and in particular, to select the best performing catalyst from the list in Table 1, we conducted a typical $^1O_2$ HDA

Table 1 List of the catalysts with their formula and literature references for preparation

Entry	Catalyst[a]	Formula[b,c]	Ref.
1	**C1**	g-C_3N_4/PEA_2PbCl_4 5%	18
2	**C2**	g-C_3N_4/PEA_2SnBr_4 5%	18
3	**C3**	g-C_3N_4/PEA_2PbBr_4 5%	18
4	**C4**	g-C_3N_4/$DMASnBr_3$ 5%	20

[a] PEA, phenylethylammonium. [b] Percentage of perovskite in g-C_3N_4 (5%). [c] DMA, dimethylammonium.

cycloaddition reaction with 1,3-cyclohexadiene using acetonitrile as a solvent, at room temperature for 24 h (Scheme 1). The conditions were the same as those used in previous experiments catalyzed by oxidized g-C_3N_4 and applied here for the sake of comparison.[15]

The choice of 1,3-cyclohexadiene is due to its reduced reactivity with respect to cyclopentadiene; this helps in limiting the potentially expected polymerization of the diene as well as side reactions under the experimental conditions. Irradiation was conducted under simulated solar light for 24 hours, saturating the acetonitrile phase with pure oxygen, and leaving the reaction under an oxygen atmosphere (using a balloon as a reservoir connected to the photochemical vessel). Table 2 reports the data relative to the different catalysts used and the yield values for the reaction at hand. In all the reactions, and as similarly done in the previous work,[15] we verified that the 1,3-cyclohexadiene conversions were quantitative by GC-MS analyses that served also for the correct detection of the reaction products and structure attribution, here and in the other reported experiments. Independent replicated experiments were performed to verify the obtained results.

Intermediate **1** represents the primary HDA cycloadduct and was never detected in all the performed experiments. 4-Hydroxycyclohex-2-en-1-one (**2**) was the only reaction product for the yields reported in Table 2. This hydroxyl ketone is a known compound derived from the reductive cleavage of the peroxide O–O bond and simultaneous oxidation of one of the hydroxy functionalities, both being pathways promoted by the catalyst; the structure was confirmed by comparison with that of authentic samples (primary standard compounds were purchased) as well as NMR characterization.[15]

Catalysts **C1–3** gave modest to good yields (Table 2, entries 1–3) of compound **2** and the best result was obtained with catalyst **C4** (Table 2, entry 4) that provided 63% yield of **2**. Catalyst **C4** ameliorated the results obtained with oxidized g-C_3N_4 alone (55% yield of compound **2**).[15]

Based on the above-illustrated results, we also investigated the behavior of cyclopentadiene to probe the scope of the reaction with a highly reactive diene, testing all the prepared catalysts. Scheme 2 shows the structures of the products obtained from the reaction of photogenerated $^1O_2$ with freshly distilled cyclopentadiene. The reaction conversion is complete although affected by an important amount of cyclopentadiene polymerization material. The composition of

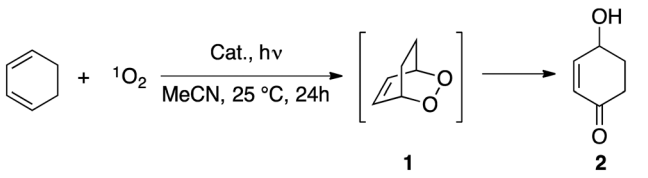

Scheme 1 HDA cycloaddition reaction of 1,3-cyclohexadiene and $^1O_2$ used as the benchmark reaction to test the efficiency of all the catalysts.

Table 2 Product **2** yields in photocatalyzed HDA reactions with 1,3-cyclohexadiene

Entry	Catalyst[a]	Product **2** (%)
1	**C1**	43
2	**C2**	26
3	**C3**	16
4	**C4**	63

[a] The amount of catalyst is 13% w/w with respect to 1,3-cyclohexadiene.

the reaction mixtures is reported in Table 3 as found by GC-MS analyses and comparison with standard references. The experimental conditions clearly activate a very fast cyclopentadiene dimerization that is responsible for the reaction outcome as shown in Scheme 2.

The primary DA cycloadduct **3** was neither isolated nor detected in the final reaction mixtures from independent experiments. Compound **4** that derives from the peroxide bond reductive cleavage was not detected too. All the reported products are known in the cited literature and the structures are consistent with the reported data.[21–29]

Catalysts of type **C1–3** showed somewhat a similar behavior with a neat preference for compound **5d** that is the bis-epoxy derivative of the cyclopentadiene dimer. Comparable amounts of the ketones **5a** and **5e** were observed (13–21%) as oxidation products of the cyclopentadiene dimer. Minor amounts of the reduction product **5c** were also observed in the range of 5–13% yield.

Ending with catalyst **C4**, the mono-epoxy derivative of the cyclopentadiene dimer **5f** was obtained in 43% yield, along with up to 10% of ketones **5a** and **b**. In all the experiments reported above, the catalyst was simply filtered at the end of each reaction and disposed. Freshly prepared catalysts were employed for new reactions and repetitions.

Oxidation of alkenes and ene reactions represent another important task where $^1O_2$ plays a pivotal role in olefin functionalization, extremely useful for the synthesis of allylic alcohols and unsaturated carbonyl compounds and, in general, value-added compounds.

The investigations in this field were conducted on a variety of alkenes, acyclic and cyclic, ranging from the highly C═C double bond substituted ones, such as tetramethylethylene (TME) and trimethylethylene (tme), to

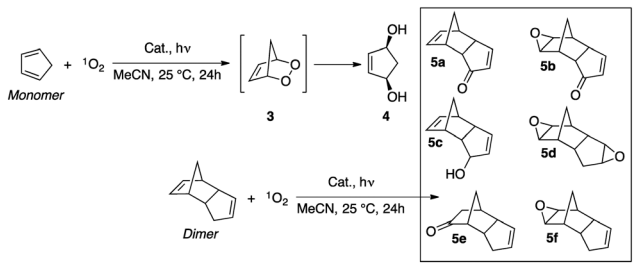

Scheme 2 HDA cycloaddition reaction of cyclopentadiene and $^1O_2$.

Table 3 Product distribution in the photocatalyzed HDA reactions with cyclopentadiene

Entry	Catalyst[a]	4 (%)	5a (%)	5b (%)	5c (%)	5d (%)	5e (%)	5f (%)
1	**C1**	—	13	—	5	30	21	—
2	**C2**	—	13	—	13	34	15	—
3	**C3**	—	16	—	7	27	13	—
7	**C4**	—	9	10	—	—	—	43

[a] The amount of catalyst is 13% w/w with respect to cyclopentadiene.

the monosubstituted ones (*e.g.* 1-octene). The studies were extended to some aromatic alkenes, such as allylbenzene, indene and dihydroanthracene. In all these cases, the reactions were performed by using the catalyst that gave the best performances in HDA cycloadditions (catalyst **C4**) under the typical set-up experimental conditions above reported.

Scheme 3 shows the results corresponding to the first series of reactions of $^1O_2$ conducted in the presence of cyclic olefins. In addition, we tested acyclic alkenes, from mono- to tetra-substituted ones with different degrees of substitution on the C=C double bond as reported in Scheme 4.

Cyclic alkenes (from 5- to 8-membered rings) gave interesting and various results that can be classified within allylic oxidation reactions such as in the cases of products **6a** and **b**, **7a** and **b**, **8b** and **9b** (Scheme 3). The product yields are fair; good performances are observed for cyclohexene where a variety of oxidized compounds were obtained with poor chemoselectivity. Some epoxydated products are often obtained in particular for 6-, 7- and 8-membered rings. Remarkably, compound **9a** was obtained in nearly 50% yield. Cyclooctene also affords compound **9c** derived from partial reductive processes. Lastly, the structures of brominated compounds **6b** and **7e** and **f** can be attributed on the basis of the presence of bromide anions in the catalysts. All the detected products are known compounds reported in the cited literature.[30–34]

On the other hand acyclic alkenes were quite unprolific (Scheme 4); the ene adduct **10**, quantitatively prepared in previous studies,[15] could not be obtained here and compound **11** was obtained in modest yields and "suffers" from the presence of bromide from the catalyst structure. Disubstituted alkenes, such as *cis*-2-hexene or *trans*-4-nonene, just to cite some of the tested olefins, did not give any positive result. In contrast, the monosubstituted 1-octene underwent oxidative pathways to afford in fair yields the diol **12a** and the ketoacid **12b**. The structures were confirmed upon comparison with known data reported in the cited literature and the used appropriate standard reference compounds.[35–37]

Representative aromatic unsaturated compounds were also tested in photocatalyzed $^1O_2$ reactions and the results are shown in Scheme 5. Indene (**13**) is prone to be oxidized with our catalytic method but the primary ene adduct **14a** was not detected in the crude reaction mixture. The diol **14b** was obtained in the reactions with catalyst **C4** in fair yields as a mixture of *cis* and *trans* isomers while ketone **14c**, a product of the direct oxidation of the sp^2 carbon atom, was also obtained. Dihydroanthracene (**15**) afforded anthraquinone **16a** in excellent yields (71%). The reaction is accompanied by the formation of anthracen-9(10*H*)-one (**16b**) (9% yield) and of anthracene (**16c**) from complete reduction of the starting material in 20% yield. Finally, we also investigated the oxidation of allylbenzene (**17**). A poorly chemoselective process results in the yields of the obtained products **18a–f**. The primary ene adduct **18a** was obtained in 3% yield using catalyst **C4**. Cinnamaldehyde (**18b**) and the corresponding alcohol **18c** are the major products along with the hydroxyl-ketone **18d**. Minor amounts of **18e** and **f** complete the mix of the products. All the compounds reported in Scheme 5 are known in the literature[38–42] and some of them were already reported in our previous work.[15]

In order to summarize, g-C_3N_4/PEA_2MX_4 composites and g-C_3N_4/$DMASnBr_3$ composites (see Table 1) were prepared and used as photocatalysts in HDA, ene and general oxidation reactions of alkenes. HDA cycloaddition reactions with 1,3-cyclohexadiene and cyclopentadiene were used to

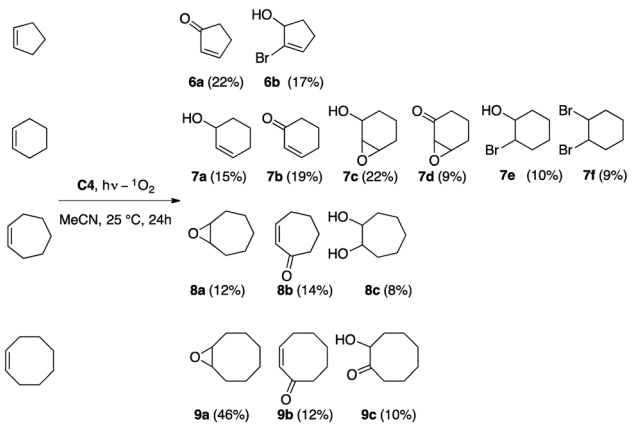

Scheme 3 Oxidation products from cyclic alkenes in $^1O_2$ photocatalyzed reactions. ND, not detected.

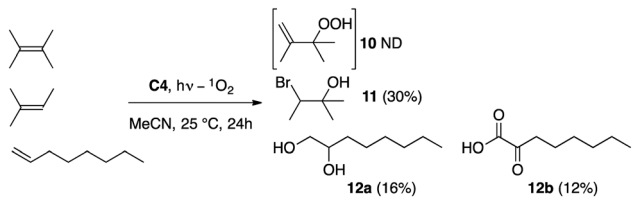

Scheme 4 Oxidation products from acyclic alkenes in $^1O_2$ photocatalyzed reactions. ND, not detected.

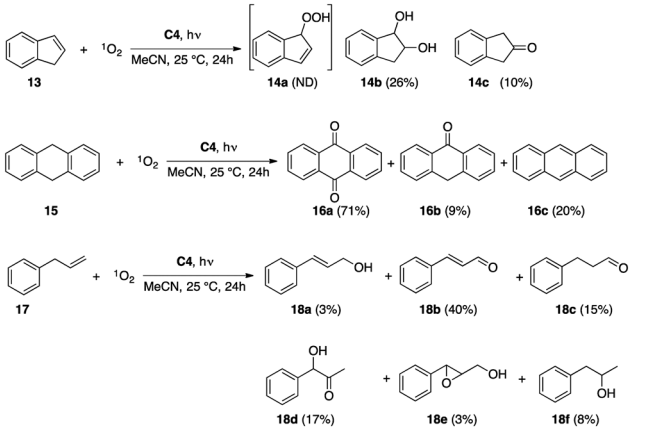

Scheme 5 Oxidation products from aromatic compounds in $^1O_2$ photocatalyzed reactions. ND, not detected.

define the best catalysts to conduct photooxidative processes with a variety of substrates. Catalyst **C4** was found to give the best results with HDA in the presence of 1,3-cyclohexadiene, affording compound **2** up to 63% yield, ameliorating our previous results obtained with simple oxidized g-C_3N_4 as the catalyst.[15]

In spite of the new catalysts employed, cyclopentadiene continues to confirm its extreme reactivity towards dimerization; this spontaneous tendency also accompanied by polymerization under the experimental conditions offers however the possibility to obtain a variety of oxidized compounds of the dimer itself.

Interesting results were obtained with cyclic alkenes of different ring sizes. The oxidation reactions are not chemoselective but α,β-unsaturated ketones are often the main products of the reactions along with the epoxides. Less promisingly, the results of acyclic alkenes do not offer a picture of the applicability of the methodology for this type of molecule, presumably not structurally fit to interact positively with the catalysts in order to give valuable oxidized compounds. Finally, aromatic compounds such as indene, dihydroanthracene and allylbenzene were easily oxidized by the selected catalysts. Specifically, catalyst **C4** did not give quantitatively anthraquinone **16a** as in our previous work[15] but still, **16a** remains the major product (up to 71%). Indene is mainly oxidized to the corresponding diol **14b** and allylbenzene offers a wide selection of oxidized compounds.

We have conducted photocatalyzed reactions with *in situ* $^1O_2$ generation in the presence of a variety of olefinic compounds. The catalysts used in the present work are substantially different from the oxidized g-C_3N_4 previously employed and offer a large matter of discussion. There are analogies and strong differences. In close similarity, catalyst **C4** (but all the catalysts in Table 1 behave similarly) displays a low chemoselectivity in the presence of some substrates or even in the absence of any reaction.

These outcomes lead to the introduction of the possibility to differentiate between photooxidation reactions of type I and type II as shown in Scheme 6.[43] Radicals or radical ions

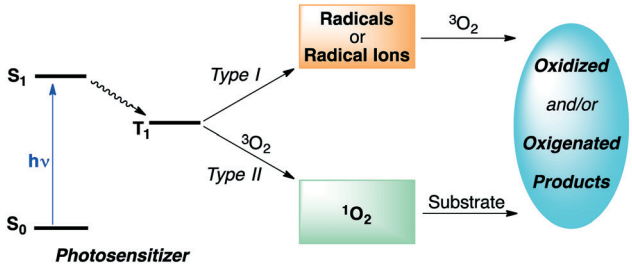

Scheme 6 Photooxidation reactions of type I and type II pathways.

can be photogenerated by suitable triplet state sensitizers and oxygen suitably trapped to give the oxidized products according to the type I photoreaction. An example is offered by the absence of any $^1O_2$ ene reactions in some of the examined reactions; the presence of other non-$^1O_2$ products such as in the indene case suggests a process promoted by a type I reaction, derived from oxygen radicals and oxygen radical ions.[44–46] On the other hand, the sensitizer promotes the $^1O_2$ formation which undergoes oxidation reactions with various substrates (type II). To discern between these two types of mechanisms, new studies are needed (chemical trap investigations) and can be reasonably planned.

Looking at Table 2, it is possible to observe that the best performing composite, providing the highest reaction yield, is the one containing $DMASnBr_3$ (**C4**). This general trend agrees with the superior photocatalytic activity observed during hydrogen photogeneration for this system relative to **C1–C3**, suggesting a direct correlation between the general activity level and the further use in HAD reactions.[18,19] On the other hand, among the 2D-based systems, the best activity is found for **C1** (PEA_2PbCl_4) which has a band-gap centered at around 3.6 eV, *i.e.* in a region where the redox potentials may even directly promote oxidation reactions. **C2** and **C3** have analogous band-gaps of around 2.7–2.8 eV and provide a direct synergy with carbon nitride (band-gap of about 2.75 eV) in terms of charge carrier transfer.[18,19] However, as we determined through computational modeling, such a positive band-alignment between the two semiconductors, namely g-C_3N_4 and the perovskite, has the maximum efficiency for **C4**, as demonstrated by the reaction yields. Let us also remember that the charge carrier lifetimes are generally longer for 3D perovskites also due to the lower binding energies, resulting in higher photocatalytic efficiencies.[20] The selectivity reported in Table 3 suggests a correlation between the type of perovskite used in the heterojunction formation (2D or 3D) and the product selectivity of the reaction. In this case, irrespective of the relative yields, 2D-based systems, both containing Br or Cl and Pb or Sn, behave similarly. In this respect, and considering the above reported arguments, it seems that the increase in catalytic activity of **C4** directly correlates with the product selectivity.

Conclusions

In conclusion, we can affirm that the g-C_3N_4/PEA_2MX_4 and g-C_3N_4/$DMASnBr_3$ composites are interesting and valuable

photocatalysts for the *in situ* generation of $^1O_2$ to perform HDA, ene and oxidation reactions with suitable dienes and alkenes. The methodology has been reasonably standardized and made applicable to a variety of olefinic substrates. The scope of the method has been finely illustrated by the results in all the tested reactions, which allowed for obtaining of desymmetrized hydroxy-ketone derivatives, unsaturated ketones and epoxides. Notable limitations were also observed especially in the case of the alkene oxidation as well as the poor chemoselectivity somewhere observed. The tuned-up oxidative properties of the suitably modified g-C_3N_4 catalysts offer a remarkable improvement in determining a change in the approach to singlet oxygen generation methods that may open other ways to perform organic reactions through greener and sustainable methodologies.

Finally, we highlight that this paper reports the first application of MHP-based composites for *in situ* generation of $^1O_2$ and that the experimental protocol applied here can be used as a platform to further expand the knowledge and applicability of MHPs to this class of organic reactions. As is well known, perovskites offer a rich variety of tuning strategies which may be explored to improve reaction yields and selectivities.

Experimental

For all the HDA, ene and oxidation reactions, the following experimental procedure was used.

Reaction method

1.4 mmol of diene or alkene substrates were dissolved in 20 mL pure acetonitrile in the presence of 15 mg of the catalyst (typically 13% w/w) in a 35 mL cylindrical Pyrex reaction vessel and the mixture was saturated with oxygen gas by bubbling for 15 minutes. The sealed vessel was then irradiated under vigorous stirring in a Solar Box Co.Fo.Me. Gra. 1500 e (500 W m^{-2}) for 24 hours. Further saturations with oxygen (a couple) were done during the reaction time. After this period of time, the suspension was filtered off to obtain a clear solution that was evaporated at moderate reduced pressure heating with a water bath at 30 °C. The residues were submitted to GC-MS analyses to determine the structures of the products and the corresponding yields. The instrument used is a Thermo Scientific DSQII single quadrupole GC/MS system (TraceDSQII mass spectrometer, Trace GC Ultra gas chromatograph, TriPlus Autosampler – Thermo Scientific®, San Jose, CA, USA).

For the product characterization of known compounds, reference standards were purchased from different chemical suppliers to be submitted to GC-MS analyses for the sake of MS spectra comparison. Being known compounds, we also took advantage of the suitable MS spectra libraries available at the CGS of the University of Pavia (*vide infra*).

Chromatography was performed on an Rxi-5Sil MS capillary column (30 m length × 0.25 mm ID × 0.25 μm film thickness, Restek, Milan, Italy) with helium (>99.99%) as a carrier gas at a constant flow rate of 1.0 mL min^{-1}. An injection volume of 1 μL was employed. The injector temperature was set at 250 °C and it was operated in split mode, with a split flow of 10 mL min^{-1}. The oven temperature was programmed from 60 °C (isothermal for 4 min) to 220 °C (isothermal for 10 min) at a rate of 10 °C min^{-1}. The mass transfer line temperature was set at 250 °C. The total GC running time was 30 min.

All mass spectra were acquired with an electron ionization system (EI, electron impact mode) with an ionization energy of 70 eV and a source temperature of 250 °C, with spectral acquisition in full scan mode over a mass range of 35–450 Da. The chromatogram acquisition, detection of mass spectral peaks and their waveform processing were performed using Xcalibur MS software version 2.1 (Thermo Scientific Inc.). Assignment of chemical structures to chromatographic peaks was based on the comparison with the databases from the GC-MS NIST Mass Spectral Library (NIST 08) and Wiley Registry of Mass Spectral Data (8th Edition) as well as for the standard samples. The percentage content of each component was directly computed from the peak areas in the GC/MS chromatogram.

Author contributions

These authors made equal contributions to this work.

Conflicts of interest

There are no conflicts to declare.

Acknowledgements

Financial support from the University of Pavia, MIUR (PRIN 2015, CUP: F12F16001350005) is gratefully acknowledged. We also thank the "VIPCAT – Value Added Innovative Protocols for Catalytic Transformations" project (CUP: E46D17000110009) for valuable financial support. Thanks are also given to the project "Scent of Lombardy" (CUP: E31B19000700007) for financial support.

Notes and references

1 A. A. Frimer, *Singlet Oxygen*, CRC Press, Boca Raton, FL, 1985, Vol. I.
2 R. W. Denny and A. Nickon, Sensitized Photooxygenationof Olefins, in *Organic Reactions*, John Wiley & Sons, Inc, Hoboken, NJ, 2011, vol. 20, pp. 133–336.
3 *Active Oxygen in Chemistry*, ed. C. S. Foote, J. S. Valentine, A. Greenberg and J. F. Liebman, Chapman&Hall, London, 1995, p. 105.
4 P. R. Ogilby, *Chem. Soc. Rev.*, 2010, **39**, 3181–3209.
5 W. Adam, S. G. Bosio and N. J. Turro, *J. Am. Chem. Soc.*, 2002, **124**, 8814–8815.
6 E. L. Clennan and A. Pace, *Tetrahedron*, 2005, **61**, 6665–6691.
7 M. N. Alberti and M. Orfanopoulos, *Chem. – Eur. J.*, 2010, **16**, 9414–9421.

8 J. M. de Souza, T. J. Brocksom, D. T. McQuade and K. T. de Oliveira, *J. Org. Chem.*, 2018, **83**, 7574–7585.
9 P. Klan and J. Wirz, *Photochemistry of Organic Compounds*, J. Wiley and Sons, Chichester, 2009, pp. 404–451.
10 R. Bonnett, *Chem. Soc. Rev.*, 1995, **24**, 19–33.
11 V. Martínez-Agramunt and E. Peris, *Inorg. Chem.*, 2019, **58**, 11836–11842.
12 M. Klaper and T. Linker, *J. Am. Chem. Soc.*, 2015, **137**, 13744–13747.
13 L. Wu, Z. Abada, D. S. Lee, M. Poliakoff and M. W. George, *Tetrahedron*, 2018, **74**, 3107–3112.
14 N. Putta, A. M. Reddy, G. Sheelu, B. V. Subba Reddy and T. Kumaraguru, *Tetrahedron*, 2018, **74**, 6673–6679.
15 I. Camussi, B. Mannucci, A. Speltini, A. Profumo, C. Milanese, L. Malavasi and P. Quadrelli, *ACS Sustainable Chem. Eng.*, 2019, **7**, 8176–8182.
16 Z. Wang, X. Hong, S. Zong, C. Tang, Y. Cui and Q. Zheng, *Sci. Rep.*, 2015, **5**, 12602.
17 K. S. Lakhi, D. H. Park, K. Al-Bahily, W. Cha, B. Viswanathan, J. H. Choy and A. Vinu, *Chem. Soc. Rev.*, 2017, **46**, 72–101.
18 L. Romani, A. Bala, V. Kumar, A. Speltini, A. Milella, F. Fracassi, A. Listorti, A. Profumo and L. Malavasi, *J. Mater. Chem. C*, 2020, **8**, 9189–9194.
19 A. Pisanu, P. Quadrelli, G. Drera, L. Sangaletti, A. Speltini and L. Malavasi, *J. Mater. Chem. C*, 2019, **7**, 7020–7026.
20 L. Romani and L. Malavasi, *ACS Omega*, 2020, **5**, 25511–25519.
21 H. Koch, J. Pirsch and A. Benedikt, *Monatsh. Chem.*, 1963, **94**, 1093–1097.
22 C.-C. Chang, J.-F. Lee and S. Cheng, *J. Mater. Chem. A*, 2017, **5**, 15676–15687.
23 C. Alvarez, R. Pelaez and M. Medarde, *Tetrahedron*, 2007, **63**, 2132–2141.
24 D. Schnurpfeil, *J. Prakt. Chem.*, 1983, **325**, 481–488.
25 S. Terashima and S. Yamada, *Tetrahedron Lett.*, 1977, 1001–1004.
26 J. Zhu, A. J. H. Klunder and B. Zwanenburg, *Tetrahedron*, 1995, **51**, 5117–5132.
27 P. P. M. A. Dolls, E. G. Arnouts, J. Rohaan, A. J. H. Klunder and B. Zwanenburg, *Tetrahedron*, 1994, **50**, 3473–3490.
28 J.-B. Wiel and F. Rouessac, *J. Chem. Soc., Chem. Commun.*, 1976, 446–447.
29 H. Ingelbrecht, A. Kumar, A. R. Menon, P. Nadkarni and R. Pawar, US2007/0049767Al, 2007.
30 M. Sankaralingam, Y.-M. Lee, W. Nam and S. Fukuzumi, *Inorg. Chem.*, 2017, **56**, 5096–5104.
31 A. A. Ponaras and O. Zaim, *J. Org. Chem.*, 1986, **51**, 4741–4743.
32 J. Yu, Y. Zhou, Z. Lin and R. Tong, *Org. Lett.*, 2016, **18**, 4734–4737.
33 S. R. Amanchi, A. M. Khenkin, Y. Diskin-Posner and R. Neumann, *ACS Catal.*, 2015, **5**, 3336–3341.
34 J. Zhang, W.-J. Wei, X. Lu, H. Yang, Z. Chen, R.-Z. Liao and G. Yin, *Inorg. Chem.*, 2017, **56**, 15138–15149.
35 H. Göksu, D. Dalmizrak, S. Akbayrak, M. S. Gültekin, S. Ozkar and O. Metin, *J. Mol. Catal. A: Chem.*, 2013, **378**, 142–147.
36 T. W. Collette, S. D. Richardson and A. D. Thruston Jr., *Appl. Spectrosc.*, 1994, **48**, 1181–1192.
37 B. You, S. Li, N. T. Tsona, J. Li, L. Xu, Z. Yang, S. Cheng, Q. Chen, C. George, M. Ge and L. Du, *ACS Earth Space Chem.*, 2020, **4**, 631–640.
38 D. Jiang, W. Hu, M. Chen, Z. Fu, A. Su, B. Yang, F. Mao, C. Zhang, Y. Liu and D. Yin, *ChemSusChem*, 2020, **13**, 1785–1792.
39 K. Raghuvanshi, C. Zhu, M. Ramezani, S. Menegatti, E. E. Santiso, D. Mason, J. Rodgers, M. E. Janka and M. Abolhasani, *ACS Catal.*, 2020, **10**, 7535–7542.
40 A. Wusiman and C.-D. Lu, *Appl. Organomet. Chem.*, 2015, **29**, 254–258.
41 M. Ju, W. Guan, J. M. Schomaker and K. C. Harper, *Org. Lett.*, 2019, **21**, 8893–8898.
42 M.-C. Lacasse, C. Poulard and A. B. Charette, *J. Am. Chem. Soc.*, 2005, **127**, 12440–12441.
43 M. S. Baptista, J. Cadet, P. Di Mascio, A. A. Ghogare, A. Greer, M. R. Hamblin, C. Lorente, S. C. Nunez, M. S. Ribeiro, A. H. Thomas, M. Vignoni and T. M. Yoshimura, *Photochem. Photobiol.*, 2017, **93**, 912–919.
44 P. A. Burns and C. S. Foote, *J. Am. Chem. Soc.*, 1974, **96**, 4339–4340.
45 P. A. Burns, C. S. Foote and S. Mazur, *J. Org. Chem.*, 1976, **41**, 899–907.
46 N. R. Easton Jr, F. A. L. Anet, P. A. Burns and C. S. Foote, *J. Am. Chem. Soc.*, 1974, **96**, 3945–3948.

